Journal of Polytechnic, 2017; 20 (1) : 9-16

On the Yielding of Two-Layer Composite Spherical Pressure Vessels

Tolga AKIŞ

Department of Civil Engineering, Atılım University, İncek-Ankara, Turkey

(Received : 23.01.2016 ; Accepted : 30.05.2016)

ABSTRACT

The yielding of two-layer composite spherical pressure vessels under either internal or external pressure is investigated analytically in the framework of small deformations and von Mises yield criterion. It is shown for both pressure cases that depending on the material properties and sphere dimensions, different modes of plasticization may take place. Unlike the deformation behavior of a single layer spherical pressure vessel, yielding may commence at the inner layer or at the outer layer or simultaneously at both layers of the assembly.

Keywords: Stress Analysis, Spherical Pressure Vessels, von Mises Criterion.

1. INTRODUCTION

The prediction of stresses in commonly used structures such as tubes, shafts, annular disks and pressure vessels is an important topic in engineering practice. The classical problem of a thick-walled spherical pressure vessel under different loading and boundary conditions has been investigated by several researchers in the past. Timoshenko and Goodier [1] derived the expressions of the stresses in a thick-walled sphere subjected to internal and external pressure. Mendelson [2] studied the elastic and elastoplastic deformation behavior of spherical pressure vessels under thermal and pressure loading. Noda et al. [3] derived the stress and displacement expressions of thick-walled spheres under various types of thermal loads. Jiang [4] studied the elastic-plastic response of such assemblies subject to internal and external pressures and radial temperature gradient. Bufler [5] investigated the laminated composite hollow spheres under pressure.

In recent years, analytical studies focusing on pressure vessels made of functionally graded materials (FGM) and multilayered pressure vessels were performed both in elastic and elastoplastic stress states. For example, Guven [6], You et al. [7], Eslami et al. [8], and Chen and Lin [9] treated the FGM spheres under different loading conditions in elastic stress state. On the other hand, Fukui and Yamanaka [10], Horgan and Chan [11], and Tutuncu and Ozturk [12] treated the internally pressurized FGM cylindrical pressure tube problem in elastic stress state. The elastoplastic response of FGM spherical pressure vessels was investigated by Akis [13], while Eraslan and Akis [14] investigated the elastoplastic response of FGM cylindrical pressure vessels, and Jahromi et. al [15, 16] studied the autofrattage of such assemblies. Besides these studies, both the mechanical and thermal stresses in the FGM cylindrical tubes were studied by several researchers such as Jabbari, Sohrabpour and Eslami [17] and Eraslan [18]. The closely related studies on the pressurized two-layer composite thick-walled tubes may be found in publications [19-22]. Finally, recent studies on spherical and cylindrical pressure vessels can be found in [23-26].

It is evident from the list of the existing literature that the investigation of the yielding behavior of the pressurized two-layer spherical pressure vessel problem by analytical means has not yet been done. It is therefore the main objective of this work to obtain a consistent analytical solution to predict the yielding behavior of such assemblies under pressure. The geometry considered in this study consists of two concentric thick spheres: A sphere layer of inner radius *a* and outer radius *b* and a sphere layer of inner radius *b* and outer radius *c*. This composite system is subjected to either internal or external pressure. The elastic behavior of the system is investigated analytically and the limiting pressures causing plastic flow are evaluated by the use of von Mises yield criterion. It is shown that, unlike the deformation behavior of a single layer spherical pressure vessel, yielding may start at the inner surface or at the interface of the assembly.

2. FORMULATION AND SOLUTION

Spherical coordinates (r, θ, ϕ) are considered in this problem. In addition, infinitesimal deformations are presumed and the notation of Timoshenko and Goodier [1] is used. For a spherical symmetric deformation case ($\sigma_\theta = \sigma_\phi$), the strain-displacement relations

$$\varepsilon_r = \frac{du}{dr}, \tag{1}$$

$$\varepsilon_\theta = \frac{u}{r}, \tag{2}$$

the Hooke's law

$$\varepsilon_r = \frac{1}{E}\left(\sigma_r - 2\nu\sigma_\theta\right), \tag{3}$$

$$\varepsilon_\theta (= \varepsilon_\phi) = \frac{1}{E}\left[\sigma_\theta - \nu(\sigma_r + \sigma_\theta)\right] \tag{4}$$

**Sorumlu Yazar (Corresponding Author)*
e-posta: tolga.akis@atilim.edu.tr
Digital Object Identifier (DOI) : 10.2339/2017.20.1 9-16

and the equation of equilibrium

$$\frac{d\sigma_r}{dr}+\frac{2}{r}(\sigma_r-\sigma_\theta)=0 \tag{5}$$

form the basis for the analysis. In these equations, ε_j represents the normal strain, *u* the radial displacement, *r* the radial coordinate, *E* the modulus of elasticity, σ_j the normal stress, and ν is the Poisson's ratio. A straight forward manipulation on the equations above leads to stress-displacement relations:

$$\sigma_r=\frac{E}{(1+\nu)(1-2\nu)}\left[2\nu\frac{u}{r}+(1-\nu)u'\right], \tag{6}$$

$$\sigma_\theta(=\sigma_\phi)=\frac{E}{(1+\nu)(1-2\nu)}\left[\frac{u}{r}+\nu u'\right], \tag{7}$$

where a prime denotes differentiation with respect to the radial coordinate *r*. Substituting the stresses from (6) and (7) in the equation of equilibrium (5) one obtains the governing differential equation for the radial displacement in a spherical pressure vessel. The general solution is

$$u(r)=\frac{C_1}{r^2}+C_2 r\,, \tag{8}$$

where C_1 and C_2 are arbitrary integration constants. The stresses are then determined as

$$\sigma_r=E\left[-\frac{2C_1}{r^3(1+\nu)}+\frac{C_2}{1-2\nu}\right], \tag{9}$$

$$\sigma_\theta=E\left[\frac{C_1}{r^3(1+\nu)}+\frac{C_2}{1-2\nu}\right]. \tag{10}$$

For a spherical pressure vessel under internal pressure, the integration constants C_1 and C_2 are determined using boundary conditions $\sigma_r(a)=-P$ and $\sigma_r(b)=0$ as

$$C_1=\frac{a^3b^3P(1+\nu)}{2(b^3-a^3)E}, \tag{11}$$

$$C_2=\frac{a^3P(1-2\nu)}{(b^3-a^3)E}. \tag{12}$$

On the other hand, if the pressure is applied externally in radial direction, the boundary conditions read $\sigma_r(a)=0$ and $\sigma_r(b)=-P$, hence C_1 and C_2 are obtained as

$$C_1=-\frac{a^3b^3P(1+\nu)}{2(b^3-a^3)E}, \tag{13}$$

$$C_2=-\frac{b^3P(1-2\nu)}{(b^3-a^3)E}, \tag{14}$$

For spherical symmetric case, the deviatoric stress tensor S_{ij} can be written as

$$[S_{ij}]=\begin{bmatrix}\sigma_r-\bar{\sigma} & 0 & 0\\ 0 & \sigma_\theta-\bar{\sigma} & 0\\ 0 & 0 & \sigma_\varphi-\bar{\sigma}\end{bmatrix}, \tag{15}$$

where $\bar{\sigma}$ is the deviatoric stress given by $\bar{\sigma}=(\sigma_r+2\sigma_\theta)/3$. The von Mises yield stress, σ_Y, may be expressed as [27]

$$\sigma_Y=\sqrt{\frac{3}{2}S_{ij}S_{ij}}\,, \tag{16}$$

and the explicit expression can be obtained as

$$\sigma_Y=\left|\sigma_r-\sigma_\theta\right|, \tag{17}$$

by carrying out summations over repeated indices. Yielding begins as soon as the yield stress σ_Y becomes greater than the uniaxial yield limit σ_0 of the material and the elastic limit load is obtained from $\sigma_Y=\sigma_0$. Studies showed that for a single layer spherical pressure vessel, the inner surface is critical for both internal and external pressure cases and yielding always commences at this surface. Hence, the elastic limit pressure P_e can be obtained from $\sigma_0=\left|\sigma_r(a)-\sigma_\theta(a)\right|$. For both cases, this limit is found as

$$P_e=\frac{2\sigma_0(b^3-a^3)}{3b^3}. \tag{18}$$

This expression is identical with the elastic limit expression given by Mendelson [2]. As an example, a steel pressure vessel (*E* = 200 GPa, ν = 0.3, σ_0 = 430 MPa) is considered. To present the numerical results, the following nondimensional variables are used: $\bar{r}=r/b$; $\bar{\sigma}_j=\sigma_j/\sigma_0$; $\bar{u}=uE/(\sigma_0 b)$; $\bar{P}=P/\sigma_0$. The inner radius of the assembly is taken as $\bar{a}=a/b=0.7$. For the internal pressure case, using Eq. (18), the elastic limit pressure is obtained as $\bar{P}_e=0.438$. Using Eqs. (11) and (12), the dimensionless integration constants are calculated as $\bar{C}_1=C_1/b^3=3.19562\times10^{-4}$, and $\bar{C}_2=C_2=1.96653\times10^{-4}$. The corresponding stresses and displacement are plotted against the nondimensional radial coordinate in Figure 1. In order to monitor the commencement of the plastic flow, the nondimensional stress variable λ_Y is introduced. In accordance with von Mises yield criterion it is obtained from $\lambda_Y=\left|\bar{\sigma}_r-\bar{\sigma}_\theta\right|$, which corresponds to the yield stress σ_Y in the plastic core. Note that $\lambda_Y=1$ at the elastic-plastic border implying onset of plasticization at that location and $\lambda_Y<1$ in the elastic region. By following the variation of λ_Y in Figure 1, it is seen that yielding commences at the inner surface of the assembly as $\lambda_Y(a)=1$. For the external pressure case, same steel assembly is considered with $\bar{a}=a/b=0.6$. The corresponding elastic limit pressure is calculated as $\bar{P}_e=0.522667$ from Eq. (18).

Using Eqs. (13) and (14), the integration constants are obtained as $\overline{C}_1 = C_1/b^3 = -2.0124\times10^{-4}$, and $\overline{C}_2 = C_2 = -5.73333\times10^{-4}$. As a result, the profiles for the stresses and displacement shown in Figure 2 are drawn. Since $\lambda_Y(a) = 1$, yielding first begins at the inner surface of the assembly.

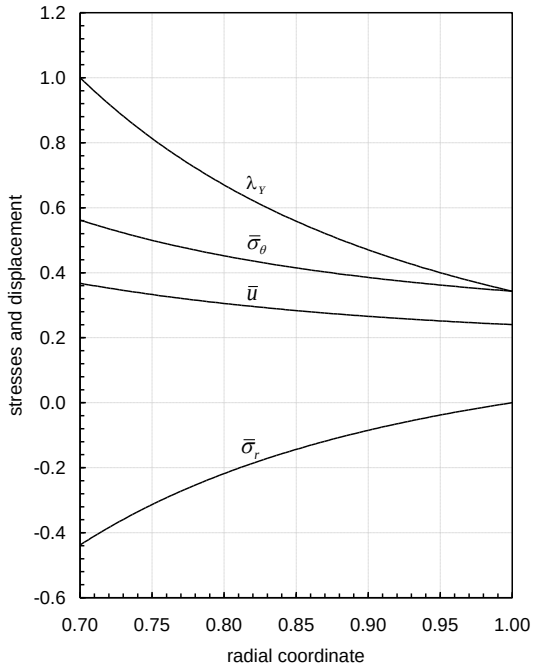

Figure 1. Stresses and displacement in a steel spherical pressure vessel of inner radius $\overline{a} = 0.7$ subject to elastic limit internal pressure $\overline{P}_e = 0.438$.

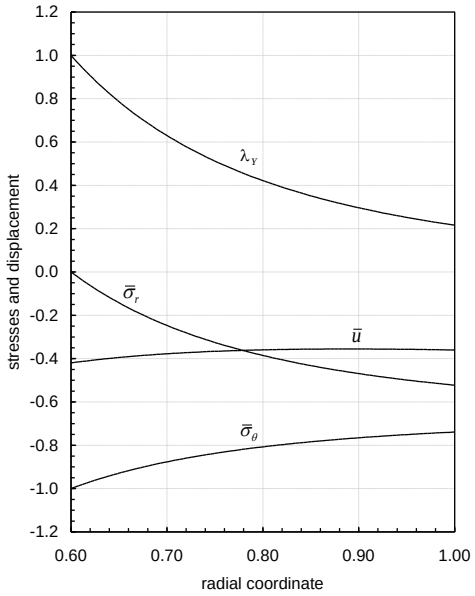

Figure 2. Stresses and displacement in a steel spherical pressure vessel of inner radius $\overline{a} = 0.6$ subject to elastic limit external pressure $\overline{P}_e = 0.522667$.

2.1 Two-Layer Assembly Subject to Internal Pressure

In two-layer composite spherical pressure vessels, same stress and displacement expressions are valid for both layers. However, these expressions contain four unknown integration constants: C_1, C_2 for the inner layer, and C_3, C_4 for the outer layer. For such an assembly subject to internal pressure *P*, these constants are determined from the boundary conditions $\sigma_r^I(a) = -P$ and $\sigma_r^{II}(c) = 0$, and the interface conditions $\sigma_r^I(b) = \sigma_r^{II}(b)$, $u^I(b) = u^{II}(b)$. Here the superscripts *I* and *II* denote inner and outer layers, respectively. The stress components and radial displacement for both layers can be obtained by the use of Eqs. (9), (10), and (8). Application of the above mentioned four nonredundant conditions results in

$$C_1 = \frac{a^3b^3PN_1\left[2(c^3-b^3)E_2M_1 + E_1(2b^3M_2 + c^3N_2)\right]}{2E_1[(c^3-b^3)E_2(2b^3M_1 + a^3N_1) + (b^3-a^3)E_1(2b^3M_2 + c^3N_2)]} \quad , \tag{19}$$

$$C_2 = \frac{a^3PM_1\left[2b^3E_1M_2 - (c^3-b^3)E_2N_1 + c^3E_1N_2\right]}{E_1[(c^3-b^3)E_2(2b^3M_1 + a^3N_1) + (b^3-a^3)E_1(2b^3M_2 + c^3N_2)]} \quad , \tag{20}$$

$$C_3 = \frac{a^3b^3c^3P(2M_1 + N_1)N_2}{2[(c^3-b^3)E_2(2b^3M_1 + a^3N_1) + (b^3-a^3)E_1(2b^3M_2 + c^3N_2)]} \quad , \tag{21}$$

$$C_4 = \frac{a^3b^3PM_2(2M_1 + N_1)}{(c^3-b^3)E_2(2b^3M_1 + a^3N_1) + (b^3-a^3)E_1(2b^3M_2 + c^3N_2)} \quad , \tag{22}$$

where

$$N_1 = 1+\nu_1, M_1 = 1-2\nu_1, N_2 = 1+\nu_2, \quad M_2 = 1-2\nu_2 . \tag{23}$$

The subscripts 1 and 2 are used to denote material properties (E, ν, σ_0) of the inner and outer layers, respectively. Parametric studies showed that, unlike the deformation behavior of a single layer pressure vessel, different modes of plastic flow may take place. Plastic deformation may first begin at $r = a$ (at the inner surface), or at $r = b$ (at the interface). These two different modes imply the existence of a critical interface radius $b = b_{cr}$ for which the plastic flow begins simultaneously in both layers. The critical interface radius b_{cr} and the corresponding elastic limit pressure P_e can be determined by simultaneous solution of the following two equations:

$$\left|\sigma_r^I(a) - \sigma_\theta^I(a)\right| = \sigma_{01} \quad , \tag{24}$$

$$\left|\sigma_r^{II}(b_{cr}) - \sigma_\theta^{II}(b_{cr})\right| = \sigma_{02} \quad . \tag{25}$$

After some algebraic manipulations, the critical interface radius b_{cr} and the corresponding elastic limit internal pressure are obtained as

$$b_{cr}=\sqrt[3]{\frac{c^3(2E_2M_1+E_1N_2)\sigma_{02}-D}{4(E_2M_1-E_1M_2)\sigma_{02}}}, \quad (26)$$

$$P_e=\frac{2\sigma_{02}}{3c^3}\left[c^3-b^3+\frac{(b^3-a^3)\left[2b^3E_1M_2+2(c^3-b^3)E_2M_1+c^3E_1N_2\right]}{a^3E_2(2M_1+N_1)}\right], \quad (27)$$

where

$$D=\sqrt{c^3\sigma_{02}\left[c^3\sigma_{02}(2E_2M_1+E_1N_2)^2-8a^3E_2\sigma_{01}(E_2M_1-E_1M_2)(2M_1+N_1)\right]}, \quad (28)$$

It is also found that the existence of the critical interface radius b_{cr} depends mainly on the material properties of the layers of the assembly. The analyses showed that, for instance, in an assembly consisting of steel inner and aluminum outer layers (ST-AL) b_{cr} exists for all a. On the other hand, in an aluminum-steel (AL-ST) assembly b_{cr} does not exist and yielding always commences at the inner surface $r=a$. If the critical interface radius exists, the plastic flow will start at the inner surface for the values of $b>b_{cr}$ and at the interface of the assembly for $b<b_{cr}$. The elastic limit internal pressure that causes yielding at the inner layer at $r=a$ is determined from Eq. (24) as

$$P_e=\frac{2\sigma_{01}}{3b^3}\left[b^3-a^3+\frac{a^3(c^3-b^3)E_2(2M_1+N_1)}{2E_2M_1(c^3-b^3)+E_1(2b^3M_2+c^3N_2)}\right]. \quad (29)$$

The equations above for the integration constants and critical pressures can easily be shown to reduce to the corresponding equations of a single layer spherical pressure vessel under internal pressure by setting $E_1=E_2=E$, $\nu_1=\nu_2=\nu$, $\sigma_{01}=\sigma_{02}=\sigma_0$ and either $a=b$ or $c=b$.

2.2 Assembly Subject to External Pressure

If the two-layer assembly is subjected to external pressure P, the boundary conditions become $\sigma_r^I(a)=0$ and $\sigma_r^{II}(c)=-P$. The interface conditions are the same as the interface conditions for the internal pressure case. Using them to determine the integration constants yields

$$C_1=-\frac{a^3b^3c^3PN_1(2M_2+N_2)}{2[(c^3-b^3)E_2(2b^3M_1+a^3N_1)+(b^3-a^3)E_1(2b^3M_2+c^3N_2)]}, \quad (30)$$

$$C_2=-\frac{b^3c^3PM_1(2M_2+N_2)}{(c^3-b^3)E_2(2b^3M_1+a^3N_1)+(b^3-a^3)E_1(2b^3M_2+c^3N_2)}, \quad (31)$$

$$C_3=-\frac{b^3c^3PN_2\left[2b^3E_2M_1-2(b^3-a^3)E_1M_2+a^3E_2N_1\right]}{2E_2[(c^3-b^3)E_2(2b^3M_1+a^3N_1)+(b^3-a^3)E_1(2b^3M_2+c^3N_2)]}, \quad (32)$$

$$C_4=-\frac{c^3PM_2\left[2b^3E_2M_1+(b^3-a^3)E_1N_2+a^3E_2N_1\right]}{E_2[(c^3-b^3)E_2(2b^3M_1+a^3N_1)+(b^3-a^3)E_1(2b^3M_2+c^3N_2)]}. \quad (33)$$

Making use of Eqs. (24) and (25), the critical interface radius and the elastic limit external pressure are obtained as

$$b_{cr}=\sqrt[3]{\frac{a^3\sigma_{01}(2E_1M_2+E_2N_1)}{E_1\left[2(\sigma_{01}+\sigma_{02})M_2+\sigma_{02}N_2\right]-2E_2\sigma_{01}M_1}} \quad (34)$$

$$P_e=\frac{2\sigma_{01}}{3}\left[\frac{c^3-b^3}{c^3}+\frac{(b^3-a^3)E_1(2M_2+N_2)}{2b^3E_2M_1-2(b^3-a^3)E_1M_2+a^3E_2N_1}\right]. \quad (35)$$

The choice $b=b_{cr}$ leads to plastic flow in both layers (at $r=a$ and $r=b$) simultaneously. Yielding commences at the interface, $r=b$, for the values of b less than b_{cr}. In case $b>b_{cr}$ or when b_{cr} does not exists, plastic flow begins at the inner surface $r=a$. The corresponding elastic limit pressure turns out to be

$$P_e=\frac{2\sigma_{02}}{3b^3}\left[b^3-a^3+\frac{(c^3-b^3)\left[2b^3E_2M_1-2(b^3-a^3)E_1M_2+a^3E_2N_1\right]}{c^3E_1(2M_2+N_2)}\right] \quad (36)$$

Like in internal pressure case, equations above for the integration constants and critical pressures can be reduced to the corresponding equations of a single layer assembly under external pressure.

3. NUMERICAL RESULTS

A composite system consisting of steel inner ($E=200$ GPa, $\nu=0.3$, $\sigma_0=430$ MPa) and aluminum outer ($E=70$ GPa, $\nu=0.35$, $\sigma_0=100$ MPa) layers is considered. To present the numerical results the following non-dimensional variables are used:

$$\bar{r}=\frac{r}{c}\ ;\ \bar{\sigma}_j=\frac{\sigma_j}{\sigma_{01}}\ ;\ \bar{u}=\frac{uE_1}{\sigma_{01}c}\ ;\ \bar{P}=\frac{P}{\sigma_{01}} \quad (37)$$

3.1 Assembly Subject to Internal Pressure

The inner radius of the assembly is taken as $\bar{a}=a/c=0.75$. In case the assembly subject to internal pressure, the critical interface radius and the corresponding critical elastic limit pressure are calculated as $\bar{b}_{cr}=b_{cr}/c=0.895058$ and $\bar{P}_e=0.318305$ using Eqs. (26) and (27), respectively. If these values are substituted in Eqs. (19)-(22) the dimensionless integration constants are obtained as $\bar{C}_1=C_1/c^3=3.93047\times10^{-4}$, $\bar{C}_2=C_2=2.99591\times10^{-4}$, $\bar{C}_3=C_3/c^3=4.60965\times10^{-4}$ and $\bar{C}_4=C_4=2.04873\times10^{-4}$. The corresponding stresses and displacement are plotted against the nondimensional radial coordinate in Figure 3(a). The radial stress and displacement are continuous at the interface satisfying interface conditions, but since the layers are made of different materials the tangential stress is discontinuous. It is also shown in this figure that the stress component σ_θ is tensile whereas σ_r is compressive. By following the variation of the

nondimensional stress variable λ_Y in Figure 3(a), it is seen that yielding commences simultaneously at the inner surfaces of both layers. For the same assembly, assigning the interface radius $\bar{b} = 0.85 < \bar{b}_{cr}$ and using Eq.(27), the elastic limit internal pressure is obtained as $\bar{P}_e = 0.235399$. The corresponding integration constants are $\bar{C}_1 = 3.30663\times10^{-4}$, $\bar{C}_2 = 2.79891\times10^{-4}$, $\bar{C}_3 = 3.94795\times10^{-4}$ and $\bar{C}_4 = 1.75464\times10^{-4}$. The distribution of stresses and displacement in the spherical pressure vessel is given in Figure 3(b). It is seen in this figure that yielding commences at the interface of the two layers since $\lambda_Y(b) = 1$. For $\bar{b} = 0.95 > \bar{b}_{cr}$, Eq. (29) gives $\bar{P}_e = 0.356688$ and from Eqs. (19)-(22) $\bar{C}_1 = 3.93047\times10^{-4}, \bar{C}_2 = 2.66582\times10^{-4}$, $\bar{C}_3 = 4.50096\times10^{-4}$ and $\bar{C}_4 = 2.00043\times10^{-4}$ are obtained. As a result, the profiles for the stresses and displacement shown in Figure 3(c) are drawn. Since $\lambda_Y(a) = 1$, yielding first begins at the inner surface of the assembly. Finally, the variation of the elastic limit internal pressure $\bar{P}_e$ with the interface radius $\bar{b}$ for steel-aluminum assembly of inner radius $\bar{a} = 0.75$ is plotted in Figure 4. Here, $\bar{b} = \bar{a} = 0.75$ implies a single aluminum spherical pressure vessel under internal pressure and the turning point of the curve corresponds to $\bar{b} = \bar{b}_{cr}$.

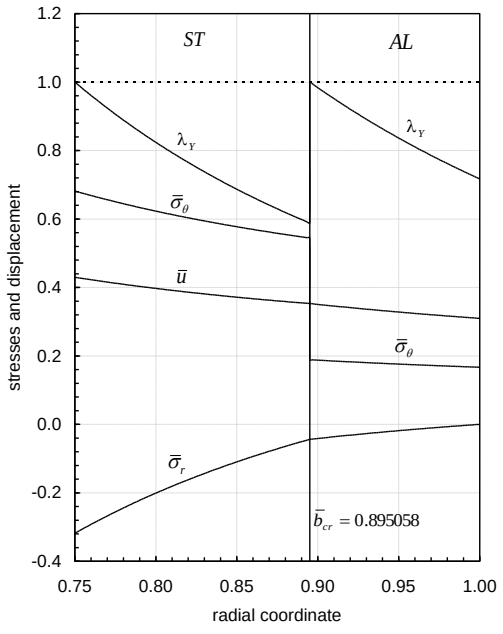

Figure 3(a). Stresses and displacement in a steel-aluminum spherical pressure vessel of inner radius $\bar{a} = 0.75$ subject to internal pressure at elastic limit internal pressure for $\bar{b} = \bar{b}_{cr} = 0.895058$ and $\bar{P}_e = 0.318305$.

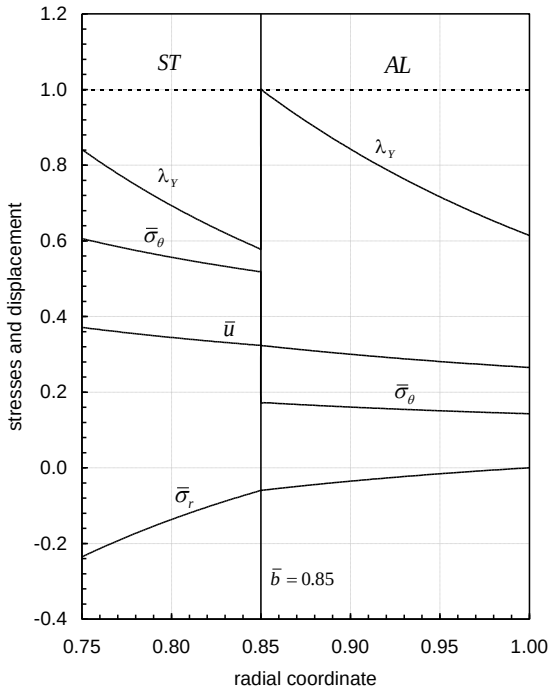

Figure 3(b). Stresses and displacement in a steel-aluminum spherical pressure vessel of inner radius $\bar{a} = 0.75$ subject to internal pressure at elastic limit internal pressure for $\bar{b} = 0.85$, $\bar{P}_e = 0.235399$

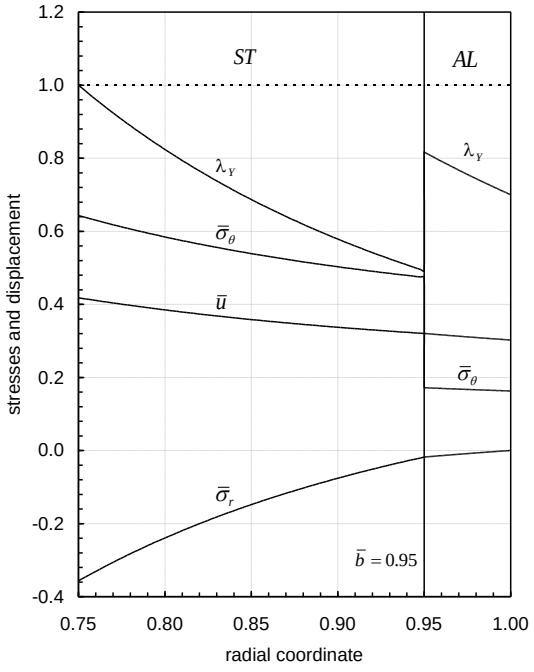

Figure 3(c). Stresses and displacement in a steel-aluminum spherical pressure vessel of inner radius $\bar{a} = 0.75$ subject to internal pressure at elastic limit internal pressure for $\bar{b} = 0.95$, $\bar{P}_e = 0.356688$.

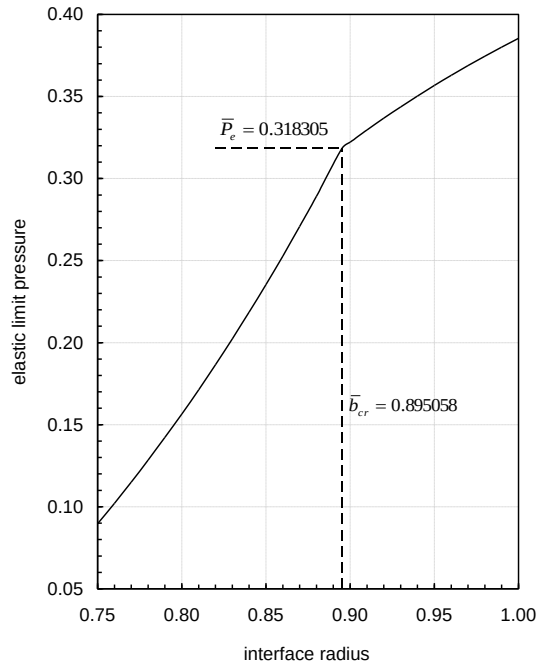

Figure 4. Variation of elastic limit internal pressure with interface radius.

3.2 Assembly Subject to External Pressure

In order to express the response of the two-layer spherical pressure vessels under external pressure, a steel-aluminum assembly is considered again. The inner radius is taken as $\bar{a} = 0.7$ and with the help of Eq. (34) the critical interface radius for this system is calculated as $\bar{b}_{cr} = 0.776302$. Using Eq. (35) for cases $\bar{b} < \bar{b}_{cr}$ and $\bar{b} = \bar{b}_{cr}$ and Eq. (36) for $\bar{b} > \bar{b}_{cr}$ and Eqs. (30)-(33) for all, calculations are performed for three different interface radii and the results are summarized in Table 1.

Table 1. Results of calculations for $\bar{a} = 0.7$

	$\bar{b} = 0.75$	$\bar{b}_{cr} = 0.776302$	$\bar{b} = 0.8$
$\bar{P}_e$	0.194742	0.260397	0.284579
$\bar{C}_1$	-2.69487×10^{-4}	-3.19562×10^{-4}	-3.19562×10^{-4}
$\bar{C}_2$	-4.83492×10^{-4}	-5.73333×10^{-4}	-5.73333×10^{-4}
$\bar{C}_3$	-2.71205×10^{-4}	-3.00751×10^{-4}	-2.80717×10^{-4}
$\bar{C}_4$	-4.79418×10^{-4}	-6.13541×10^{-4}	-6.49202×10^{-4}

The stresses and displacement corresponding to $\bar{b} = 0.75$, $\bar{b} = \bar{b}_{cr} = 0.776302$ and $\bar{b} = 0.8$ at their elastic limit external pressures are calculated and plotted in Figures 5(a), (b) and (c), respectively. As seen in these figures, both stress components are compressive. Furthermore, yielding commences in the assembly of interface radius $\bar{b} = 0.75$ in the outer layer (Figure 5(a)), simultaneously in both layers for $\bar{b} = \bar{b}_{cr} = 0.776302$ (Figure 5(b)) and in the inner layer for $\bar{b} = 0.8$ (Figure 5(c)). Finally, the variation of elastic limit external pressure $\bar{P}_e$ with the interface radius $\bar{b}$ can be seen in Figure 6.

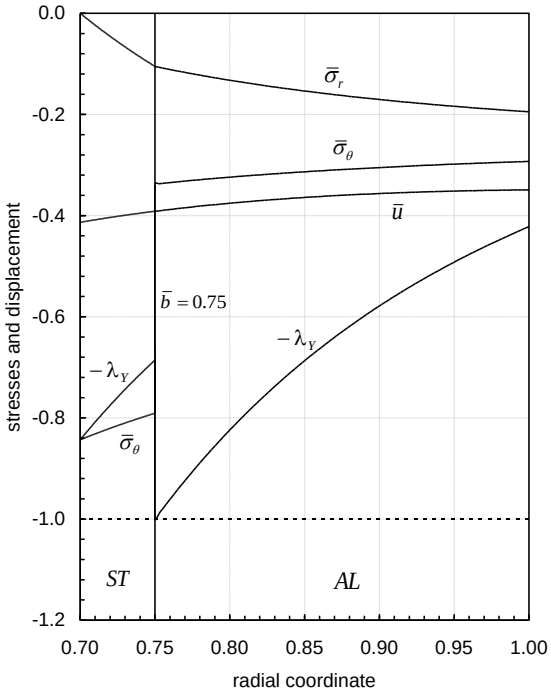

Figure 5(a). Stresses and displacement in a steel-aluminum spherical pressure vessel of inner radius $\bar{a} = 0.7$ subject to external pressure at elastic limit external pressure for $\bar{b} = 0.75$, $\bar{P}_e = 0.194742$.

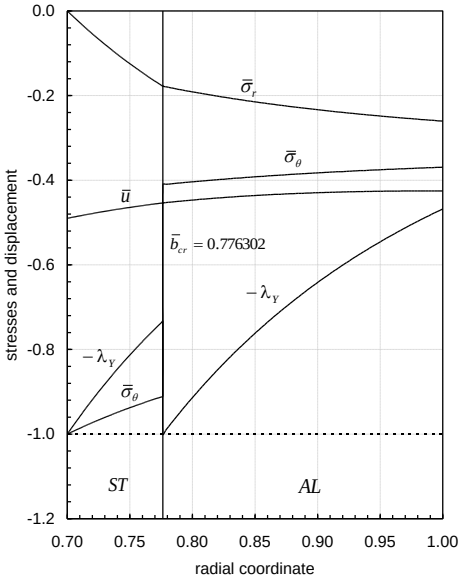

Figure 5(b). Stresses and displacement in a steel-aluminum spherical pressure vessel of inner radius $\bar{a} = 0.7$ subject to external pressure at elastic limit external pressure for $\bar{b} = \bar{b}_{cr} = 0.776302$, $\bar{P}_e = 0.260397$.

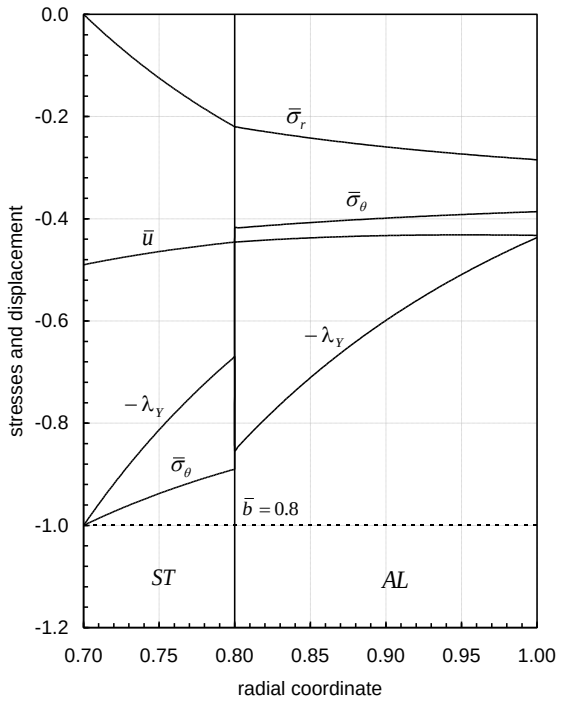

Figure 5(c). Stresses and displacement in a steel-aluminum spherical pressure vessel of inner radius $\bar{a} = 0.7$ subject to external pressure at elastic limit external pressure for $\bar{b} = 0.8$, $\bar{P}_e = 0.284579$.

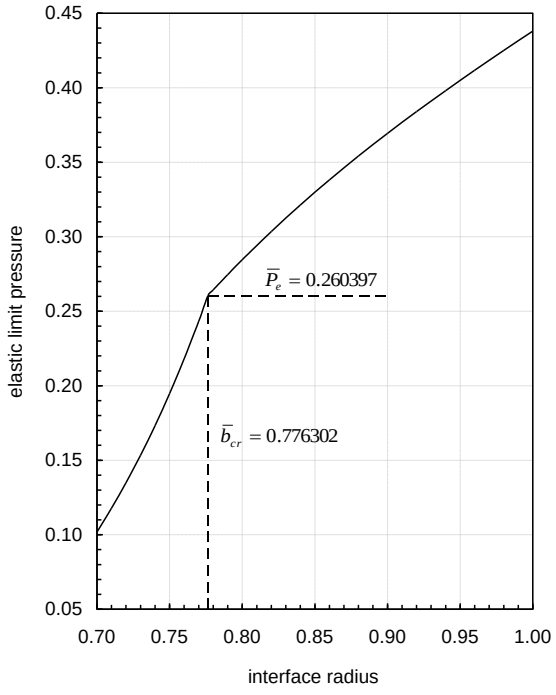

Figure 6. Variation of elastic limit external pressure with interface radius.

4. CONCLUDING REMARKS

In the framework of small deformation theory and von Mises yield criterion, an engineering stress analysis is performed in this study concerning the yielding of two-layer spherical pressure vessels under pressure. In a single layer spherical pressure vessel, the inner surface is critical regardless of internal or external pressure is applied and yielding commences at this location when the pressure reaches its elastic limit. However, in two-layer composite spherical pressure vessels, depending on the material properties and interface radius, yielding may begin in the inner layer or in the outer layer or simultaneously in both layers. A critical interface radius $\bar{b}_{cr}$ leading to plastic flow simultaneously in both layers may be found. The existence of b_{cr} mainly depends on the material properties of the layers. The plastic flow starts from the inner layer at $r = a$ if $b > b_{cr}$, it yields in the outer layer at the interface otherwise. In case b_{cr} does not exist, the assembly behaves like a single layer spherical pressure vessel.

LIST OF SYMBOLS

a, b, c	inner, interface and outer radii of the spherical pressure vessel assembly, respectively
C_i	integration constants
E	modulus of elasticity
P	pressure
r, θ, ϕ	spherical coordinates
S_{ij}	deviatoric stress tensor
u	radial displacement
ε_i	strain components
ν	Poisson's ratio
σ_i	stress components
σ_0, σ_Y	initial and subsequent yield stress
$\bar{\sigma}$	deviatoric stress
λ_Y	nondimensional stress variable

REFERENCES

1. Timoshenko S.P., Goodier J.N., "Theory of Elasticity", 3rd ed., ***McGraw-Hill***, New York, (1970).
2. Mendelson A., "Plasticity: Theory and Application", ***Macmillan***, New York, (1968).
3. Noda N., Hetnarski R.B., Tanigawa Y.,"Thermal Stresses", 2nd ed., ***Taylor and Francis***, New York, (2003).
4. Jiang W., "Hollow spheres subjected to sustained and variable loads", ***Journal of Engineering Mechanics-ASCE***, 120: 1343-1368, (1994).
5. Bufler H., "The arbitrarily and periodically laminated elastic hollow sphere: Exact solutions and homogenization", ***Archive of Applied Mechanics***, 68: 579-588, (1998).

6. Guven U., "On stress distributions in functionally graded isotropic spheres subjected to internal pressure", ***Mechanics Research Communications***, 28: 277-281, (2001).
7. You L.H., Zhang J.J., You X.Y., "Elastic analysis of internally pressurized thick-walled spherical pressure vessels of functionally graded materials", ***International Journal of Pressure Vessels and Piping***, 82: 347-354, (2005).
8. Eslami M.R., Babaei M.H., Poultangari R., "Thermal and mechanical stresses in a functionally graded thick sphere", ***International Journal of Pressure Vessels and Piping***, 82: 522-527, (2005).
9. Chen Y.Z., Lin X.Y., "Elastic analysis for thick cylinders and spherical pressure vessels made of functionally graded materials", ***Computational Materials Science***, 44: 581-587, (2008).
10. Fukui Y., Yamanaka N., "Elastic analysis for thick-walled tubes of functionally graded material subjected to internal pressure", ***The Japan Society of Mechanical Engineers***, 35: 379-385, (1992).
11. Horgan C.O., Chen A.M., "The pressurized hollow cylinder or disk problem for functionally graded isotropic linearly elastic materials", ***Journal of Elasticity***, 55: 43-59, (1999).
12. Tutuncu N.," Stress in thick-walled FGM cylinders with exponentially-varying properties", ***Engineering Structures***, 29: 2032-2035, (2007).
13. Akis T., "Elastoplastic analysis of functionally graded spherical pressure vessels", ***Computational Materials Science***, 46: 545-554, (2009).
14. Eraslan A.N., Akis T., "Plane strain analytical solutions for a functionally graded elastic-plastic pressurized tube", ***International Journal of Pressure Vessels and Piping***, 83: 635-644, (2006).
15. Jahromi B.H., Farrahi G.H., Maleki M., Hashemi H.N., Vaziri A., "Residual stresses in autofrettaged vessel made of functionally graded material", ***Engineering Structures***, 31: 2930-2935, (2009).
16. Jahromi B.H., Ajdari A., Hashemi H.N., Vaziri A., "Autofrettage of layered functionally graded metal-ceramic composite vessels", ***Composite Structures***, 92: 1812-1822, (2010).
17. Jabbari M., Sohrabpour S., Eslami M.R., "Mechanical and thermal stress in a functionally graded hollow cylinder due to radially symmetric loads", ***International Journal of Pressure Vessels and Piping***, 79: 493-497, (2002).
18. Eraslan A.N., "Stresses in FGM pressure tubes under non-uniform temperature distribution", ***Structural Engineering and Mechanics***, 26: 393-408, (2007).
19. Eraslan A.N., Akis T., "Deformation analysis of elastic-plastic two layer tubes subjected to pressure: An analytical approach", ***Turkish Journal of Engineering and Environmental Sciences***, 28: 261-268, (2004).
20. Eraslan A.N., Akis T., "Yielding of two-layered shrink-fitted composite tubes subjected to radial pressure", ***Forschung im Ingenieurwesen***, 69: 187-196, (2005).
21. Eraslan A.N., Akis T., "Stress analysis in strain hardening two-layer composite tubes subject to cyclic loading of internal pressure", ***International Journal of Advances in Applied Mathematics and Mechanics,*** 3: 65-76, (2015).
22. Eraslan A.N., Akis T., Akis E., "Deformation analysis of two-layer composite tubes under cyclic loading of external pressure", ***Journal of Basic and Applied Research International***, 13: 107-119, (2016).
23. Ghannad M., Zamaninejad M., "Complete closed-form solution for pressurized heterogeneous thick spherical shells", ***Mechanika***, 18: 508-516, (2012).
24. Sonachalam M., Ranjit Babu B.G., "Optimization of composite pressure vessel", ***International Journal of Science and Research***, 4: 1668-1670, (2013).
25. Prakash K.S.J., Mastanaiah T., "Industrial spherical pressure vessel design and analysis using FEA", ***International Journal of Computational Engineering Research***, 4: 32-35, (2014).
26. Anani Y., Rahimi G.H., "Stress analysis of thick pressure vessels composed of functionally graded incompressible hyperelastic materials", ***International Journal of Mechanical Sciences***, 104: 1-7, (2015).
27. Hill R., "The Mathematical Theory of Plasticity", ***Clarendon Press***, Oxford, (1950).